Thyroid Capsular Elastic Fiber Fragmentation as a Non-Invasive Surrogate for Capsular Invasion

Inas Abd Al Majed Rasheed[1]*, Amrah Mohammed Saeed Khudhur[2], Aiad Abdullah Abdulrazak[3]

[1]Department of pathology, College of medicine, Tikrit University, Baghdad, Iraq.
ORCID iD: https://orcid.org/0000-0002-0726-4178, Email: dr.enas11@tu.edu.iq
[2]Department of physiology, Tikrit University, Tikrit, Iraq.
[3]Department of pathology, College of medicine, Tikrit University, Tikrit, Iraq.

Abstract

Background: In encapsulated follicular-patterned thyroid tumors, proving capsular invasion requires exhaustive capsule submission, which is labor intensive and reproducible to varying degrees. We tested whether a Capsular Elastic Fiber Fragmentation Score (CEFFS), derived from Verhoeff–Van Gieson–stained sections, could serve as a histology-only surrogate for capsular invasion. **Methods:** In a single-center, blinded accuracy study, we identified 50 cases (25 minimally invasive follicular thyroid carcinoma [MI-FTC], 25 follicular adenoma [FA]) defined by WHO 2022 criteria. Two pathologists, blinded to diagnosis, selected three capsule hotspots per case and scored elastic fiber continuity loss, fragmentation proportion, and tangential re-orientation. Hotspot sums were averaged to yield CEFFS (range 0–9). Demographics were compared after Shapiro–Wilk normality checks using Welch's t-test or Mann–Whitney U for continuous variables and Fisher's exact test for sex. Group differences in CEFFS and capsule thickness used Welch's t-tests; category distributions were compared using chi-square tests. Logistic regression related MI-FTC probability to CEFFS; performance was summarized by area under ROC curve (AUC, DeLong 95% CI), calibration intercept and slope, and Brier score with 3,000 bootstrap resamples. **Results:** Groups were demographically balanced. CEFFS was higher in MI-FTC than in FA, and each 1-point increase in CEFFS approximately doubled the odds of MI-FTC (odds ratio 2.34). The CEFFS-based model showed good discrimination between MI-FTC and FA (AUC 0.87). Capsule thickness and pericapsular fibroinflammatory reaction were also greater in MI-FTC than in FA. **Conclusions:** Quantified elastic fiber disruption robustly distinguishes MI-FTC from FA and provides high-discrimination risk estimates in this single-center accuracy study. Within existing WHO/CAP diagnostic frameworks, CEFFS could be implemented as a histology-only triage tool to flag cases that warrant full circumferential capsule submission or intensified level sampling. This approach has the potential to accelerate reporting when exhaustive sampling is impractical, but validation and reproducibility studies, including external multicenter cohorts, are warranted.

Keywords: Thyroid Encapsulated Follicular Tumor, Capsular Invasion, Non-invasive Surrogate.

Introduction

Encapsulated follicular-patterned thyroid tumors, including minimally invasive follicular thyroid carcinoma (MI-FTC) and follicular adenoma (FA), are now stratified by the 2022 WHO classification into MI, encapsulated angioinvasive, and widely invasive types, while excluding noninvasive follicular thyroid neoplasm with papillary-like nuclear features (NIFTP) due to its indolent behavior.[1] This reclassification enhances risk stratification and reflects the prognostic significance of vascular invasion.[2]

Capsular and vascular invasion determine malignancy and guide therapy—total thyroidectomy and radioactive iodine therapy are recommended for angioinvasive types, while MI-FTC without vascular invasion may only need lobectomy.[3] The current diagnostic gold standard involves exhaustive capsule submission and synoptic reporting per CAP protocols.[4]

However, this method is limited by heavy sampling workload, diagnostic delays, and poor interobserver reproducibility in recognizing true invasion.[5] Hence, there is a need for a reproducible histologic surrogate for capsular invasion. Emerging tools include transcription factor profiling,[3] capsule thickness measurements,[6] and CD26 dot-like staining patterns,[7] each offering potential surrogate markers for invasion status.

The extracellular matrix (ECM), especially elastic

Access This Article Online

Quick Response Code:

Website: www.jnsbm.org

DOI: https://doi.org/10.5281/zenodo.19550061

Address for Correspondence: Department of pathology, College of medicine, Tikrit University, Baghdad, Iraq
Email: dr.enas11@tu.edu.iq

Submitted: 05th December, 2025 **Received:** 10th December, 2025
Accepted: 07th February, 2026 **Published:** 11th February, 2026

How to Cite This Article: Rasheed I A A M, Khudhur A M S, Abdulrazak, A A. Thyroid Capsular Elastic Fiber Fragmentation as a Non-Invasive Surrogate for Capsular Invasion. J Nat Sc Biol Med 2026;17(1):18-29

fibers, plays a crucial role in maintaining capsular integrity and resisting tumor invasion.[8] Compared to collagen, elastic fibers provide resilience and are uniquely vulnerable to enzymatic degradation and fragmentation during malignancy progression.[9] VVG or EVG staining techniques highlight these fibers and reveal patterns of fragmentation, thinning, and reorientation in invasive zones.[10] Disruption of elastic continuity—visible as fiber breaks or curled morphology—correlates with early capsular invasion, often before histologic breach is confirmed.[11] The Capsular Elastic Fiber Fragmentation Score (CEFFS) quantifies these changes using predefined hotspot selection rules and fragmentation severity metrics.[12] CEFFS may guide triage decisions on capsule submission or prompt surgical counseling, such as considering completion thyroidectomy.[13] For reproducibility, CEFFS demands consistent field selection, validated staining protocols, and quality control in interpretation.[14]

This study was designed to determine whether a composite Capsular Elastic Fiber Fragmentation Score derived from Verhoeff–Van Gieson–stained sections distinguished minimally invasive follicular thyroid carcinoma from follicular adenoma in encapsulated follicular-patterned tumors. We aimed to quantify the diagnostic performance of this score, expressed as its discrimination and calibration, and to estimate operating characteristics that would be meaningful in practice, including sensitivity, specificity, and likelihood ratios across clinically plausible thresholds. By focusing on elastic fiber continuity, fragmentation proportion, and tangential re-orientation averaged across predefined hotspots, we sought to test the hypothesis that microscopic patterns of elastic disruption within the capsule mirrored true capsular invasion and could serve as a practical surrogate when exhaustive capsule submission was not feasible.

We further aimed to evaluate the reproducibility of the scoring approach between two blinded pathologists and to report agreement statistics for the composite score and its individual components. Because capsule biology and peri-capsular stromal responses might confound or inform the interpretation of elastic changes, we also set out to examine associations between the score and capsule thickness as well as the surrounding fibroinflammatory reaction. These analyses were planned to clarify whether the proposed metric captured invasion-related mechanics rather than nonspecific stromal alterations.

Finally, we aimed to assess the potential clinical utility of the score by conducting misclassification cost analyses and decision-curve analyses to estimate net benefit across thresholds relevant to surgical counseling and the consideration of completion thyroidectomy. Internal bootstrap validation was planned to quantify optimism in model estimates and to judge the stability of performance metrics in a sample of limited size. Through these objectives, the study sought to provide an evidence-based, purely histologic tool that could shorten turnaround time, reduce the burden of exhaustive capsule submission, and inform immediate clinical decision-making without reliance on imaging.

Methodology

Study Setting and Blinded Controlled Design

The study was conducted within a single tertiary academic anatomic pathology service that processed thyroidectomy specimens under ISO-compliant workflows. All slide labels were replaced with study IDs and QR codes generated from a computer-randomized list prior to review, and case packets excluded gross descriptions, radiology, and clinical notes to preserve blinding. Two attending pathologists reviewed each case independently in separate sessions; slide order was randomized per case to minimize order effects. The control arm comprised follicular adenomas verified by exhaustive capsule submission, while the study arm comprised minimally invasive follicular thyroid carcinomas verified by the reference standard described below. Blinding integrity was monitored by audit logs in the electronic database and by spot checks of slide relabeling. Synoptic documentation followed the College of American Pathologists (CAP) thyroid carcinoma protocol to standardize case summaries without revealing original diagnoses during reads. Electronic data capture used REDCap hosted on a secure institutional server with role-based permissions; only a data manager had access to the key linking study IDs to medical record numbers. The controlled design enabled a fixed 1:1 allocation (25 MI-FTC, 25 FA) and ensured that no imaging, gross photographs, or operative reports were available to raters during scoring. CAP synoptic guidance and REDCap's audit trail supported protocol fidelity and masking throughout acquisition and review.[15]

Case Ascertainment and Eligibility for Encapsulated Follicular-patterned Tumors

Eligible cases were archival, encapsulated follicular-patterned thyroid tumors resected during routine clinical care, fixed and processed under standard conditions, with complete clinical follow-up available for chart abstraction after the blinded reads. Inclusion criteria required a discrete, grossly circumscribed nodule with a continuous fibrous capsule and predominant follicular architecture without diagnostic nuclear features of papillary thyroid carcinoma. Exclusions encompassed noninvasive follicular thyroid neoplasm with papillary-like nuclear features (NIFTP), poorly differentiated thyroid carcinoma, widely invasive follicular carcinoma, oncocytic (Hürthle/oncocytic) neoplasms when ≥75% oncocytic cells were present, metastatic disease to thyroid, prior radioiodine therapy before resection, and any case with suboptimal fixation precluding elastic staining. Tumor size, multifocality, and background thyroid disease did not determine eligibility provided encapsulation and architecture criteria were met. Where oncocytic change did not reach the 75% threshold, cases were retained and annotated for sensitivity analyses. Eligibility gates reflected the 5th edition WHO

classification framework separating minimally invasive FTC from encapsulated angioinvasive FTC and from benign counterparts, to reduce heterogeneity and align with contemporary diagnostic conventions. These definitional boundaries were applied before blinding and were documented in a prespecified screening log.[16]

Reference Standard for MI-FTC Versus FA Classification

The reference standard adhered to WHO 2022 criteria. Minimally invasive follicular thyroid carcinoma was defined as an encapsulated follicular neoplasm demonstrating unequivocal microscopic capsular invasion and/or limited vascular invasion, with the extent of invasion not meeting criteria for widely invasive disease. Encapsulated angioinvasive tumors were classified separately when vascular invasion was present, with limited versus extensive vascular involvement stratified by the number of invaded vessels (<4 vs ≥4) to guide management context; such cases were not used as FA controls. Follicular adenoma required a completely encapsulated follicular-patterned tumor without capsular or vascular invasion after exhaustive capsule submission and step-sectioning as per local practice, with synoptic reporting based on CAP protocol language. All reference calls were established by consensus outside the blinded scoring sessions, using all available histologic levels and the full capsule sampling record; no elastic stain features were considered in the reference call. These definitions were grounded in WHO updates and CAP documentation to ensure contemporary classification and reproducibility across centers.[16]

Sample Size Justification and Fixed Allocation (25 MI-FTC, 25 FA)

The fixed 1:1 allocation of 25 MI-FTC and 25 FA cases was justified a priori for discrimination analysis centered on the area under the ROC curve (AUC). Using the Hanley–McNeil variance approximation for AUC under a binormal assumption and external tools that implement those formulas, a total sample of 50 with equal groups provides workable precision for an anticipated AUC in the 0.80 range versus the null AUC of 0.50 at two-sided α=0.05, yielding approximate power near conventional thresholds while maintaining feasibility for a special-stain histology workflow. We planned to quantify the AUC and its confidence intervals with the pROC package and, if desired, corroborate planning estimates through power.roc.test and comparable sample-size utilities that implement Obuchowski/McClish developments. Because the study was designed as a controlled, single-center accuracy study with no imaging or molecular stratification, we set the allocation to fix the disease:non-disease ratio at 1:1 to stabilize variance across CEFFS thresholds and facilitate internal bootstrap validation. The final total of 50 also aligns with published guidance showing that small to moderate ROC studies can obtain interpretable precision when design effects are minimized by blinding and standardized protocols.[17]

Specimen Retrieval, Processing, and Slide Selection (H&E and VVG)

Formalin-fixed paraffin-embedded blocks were retrieved from archives. Tissue had been fixed in 10% neutral buffered formalin (NBF), which corresponds to ~4% w/v formaldehyde buffered to pH ~7.0, the diagnostic standard for surgical pathology fixation. Processing used a programmable tissue processor with paraffin infiltration; representative devices included Leica ASP300 S, which supported controlled pressure/vacuum cycles and reagent management. Embedding used Paraplast Plus® paraffin (Sigma-Aldrich P3683; melting point 56–57 °C), and blocks were sectioned at 4 µm on a rotary microtome (e.g., Leica RM2235; section thickness setting range 1–60 µm). Sections were mounted on positively charged slides to enhance adhesion, using Fisherbrand™ Superfrost™ Plus (Cat. 12-550-15 or 22-037-246), and coverslipped with #1.5 cover glass of 0.16–0.19 mm thickness; permanent mounting employed Cytoseal™ XYL (Thermo Scientific Cat. 8312-4 or equivalent). Routine H&E used Gill's hematoxylin (e.g., Sigma GHS232/GHS280) and eosin Y solutions per manufacturer instructions. For elastic staining, additional unstained levels were cut and reserved for the VVG protocol as detailed below. Slide adequacy required intact capsule representation on at least three distinct circumferential segments and absence of processing chatter across the capsule plane. (MilliporeSigma)

Verhoeff–Van Gieson Elastic Staining Protocol and Quality Assurance

Elastic fibers were demonstrated using a standardized Verhoeff–Van Gieson (VVG/EVG) stain kit. Validated commercial kits included MasterTech/StatLab Verhoeff's Elastic Stain Kit (e.g., Item KTVELPT; IFU lists components 5% alcoholic hematoxylin, 10% ferric chloride, iodine, 5% sodium thiosulfate, Van Gieson's), Polysciences VVG Elastin Stain Kit (Product No. 25089), and Abcam Elastic Stain Kit (ab150667). Following the IFU, sections were overstained in Verhoeff's working solution, differentiated in ferric chloride to a gray background, treated with sodium thiosulfate, and counterstained with Van Gieson to yield black elastic fibers against red collagen and yellow background; typical kit protocols produced diagnostic staining in ~20 minutes, and 100 mL kits yielded ~36–45 slides. Each daily batch included a positive control (aorta control slide, e.g., CSA0825P) and a negative-tissue internal control. Storage and quality criteria followed vendor guidance (e.g., 15–30 °C, tamper-evident seals); runs failed QC if elastic fibers were under- or over-differentiated, collagen was not crimson, or nuclear detail was obscured. Lot numbers, expiration dates, and differentiation endpoints were logged; unsuccessful batches were repeated with titrated differentiation times before any scoring.[18]

Hotspot Identification along the Capsule and Field Selection Rules

Hotspots were operationalized as capsule segments showing the greatest disruption of elastic fiber continuity

at screening magnification, then confirmed at higher power for scoring. The tumor–capsule interface was first surveyed at low power to map the full circumference, avoiding knife-chatter zones or folds. Three non-overlapping hotspots were then sampled along distinct capsule quadrants with at least 1 mm linear separation between fields. Field geometry was standardized using a 10× eyepiece with 22 mm field number and a 20× objective, yielding an on-specimen field diameter of ~1.1 mm and area of ~0.95 mm²; this provided consistent sampling window sizes across cases. When the capsule exceeded one field, the field center was anchored on the most disrupted region while ensuring complete inclusion of the capsule thickness from thyroid side to extrathyroidal side. Tangential cutting artifacts were excluded by cross-checking serial levels. If the capsule was focally absent due to prior sectioning, the nearest intact continuous segment was chosen to maintain comparability. All field selections were recorded in the database with XY stage coordinates and a brief rationale entered contemporaneously to support auditability without revealing diagnoses during scoring.[19]

Definition and Computation of the Capsular Elastic Fiber Fragmentation Score (CEFFS)

CEFFS was defined as the unweighted mean of three ordinal subcomponents scored independently within each hotspot and then averaged across three hotspots per case. Fiber continuity loss captured macroscopic gaps within the elastic lamina across the capsule thickness, scored as 0 (none), 1 (microfissures confined to ≤10% of the capsule span), 2 (multifocal discontinuities affecting >10% and ≤50%), or 3 (segmental/full-thickness breaks affecting >50%). Fragmentation proportion reflected the percentage of elastic fibers present as discrete fragments rather than continuous strands within the capsule plane, scored as 0 (≤5%), 1 (6–25%), 2 (26–50%), or 3 (>50%). Tangential re-orientation quantified deviation of elastic fibers from the expected circumferential/radial alignment, measured as the dominant angle of misalignment relative to the capsule axis: 0 (<15°), 1 (15–30°), 2 (31–45°), 3 (>45°). Each hotspot's subcomponent scores were summed (0–9), then averaged across three hotspots to yield a CEFFS from 0 to 9 at 0.01 resolution. The scoring rubric, with photomicrographic exemplars prepared during training, prioritized structural damage over staining intensity; intensity variation alone without structural change did not increase CEFFS. No external diagnostic information was permitted during scoring.

Measurement of Secondary Capsular Metrics: Thickness and Pericapsular Fibroinflammatory Reaction

Capsule thickness was measured orthogonally across the narrowest capsule span at five equidistant points within each preselected hotspot, using calibrated image-analysis tools after objective-specific calibration with a 1 mm/100-division stage micrometer (0.01 mm per division). Calibration checks were logged daily before measurements. Thickness values were recorded in millimeters to three decimals and summarized as the hotspot mean; the case-level thickness summarized the mean of three hotspot means. Pericapsular fibroinflammatory reaction was scored on adjacent H&E sections as 0 (absent to rare fibroblasts, no perivascular lymphocytes), 1 (mild fibroblast proliferation and sparse perivascular lymphocytes without storiform change), or 2 (dense fibroblastic reaction and perivascular lymphoid aggregates contiguous with the capsule). Edge artifacts, retraction spaces, and cautery-induced stromal changes were excluded by cross-referencing serial levels. Measurements were performed only when section orientation preserved a perpendicular capsule profile; oblique sections were flagged and not measured at that point. All metric entries were time-stamped in the database with the calibration record ID to ensure traceability.[20]

Pathologist Training Set, Calibration Exercise, and Blinding Procedures

Before scoring, both pathologists completed a calibration exercise using 10 pilot cases not included in the main sample. The exercise included review of annotated examples for each CEFFS subcomponent with agreed-upon visual thresholds, followed by independent scoring and a structured adjudication session to harmonize interpretations. Training materials incorporated CAP synoptic elements for consistent terminology and used screenshots from the institution's imaging software to illustrate measurement placement; however, these materials contained no diagnostic labels and were stored separately from the scoring workspace. Case packets for the main study were assembled by a coordinator who performed relabeling and randomization; slide cassettes were recoded and the key file was maintained offline. REDCap user roles restricted access such that only the data manager could view the allocation list; raters saw only the de-identified case ID and scoring forms. Blinding was reinforced by disabling access to clinical systems during read sessions. Adherence checks included periodic verification that control positive aorta slides and kit lot numbers were recorded without linking to case identity.[15]

Interobserver Reproducibility Assessment and κ Statistics Plan

Reproducibility of CEFFS and its subcomponents was assessed with Cohen's weighted κ using linear weights to respect the ordinal nature of the 0–3 categories. For the case-level CEFFS (0–9 continuous mean), agreement was additionally summarized by intraclass correlation (two-way random, absolute agreement) as a sensitivity analysis, but κ on categorized CEFFS thresholds remained the primary reliability metric for clinical cutpoints. Ninety-five percent confidence intervals for κ were obtained via percentile bootstrap with 2,000 resamples to avoid reliance on large-sample asymptotics in a modest dataset. Interpretation of κ magnitudes followed conventional gradations described by Landis and Koch, without

imposing hard clinical thresholds. Where subcomponent marginals were highly imbalanced, we planned to report prevalence- and bias-adjusted κ alongside the primary estimate. Discrepancy resolution for the final analysis set used the mean of raters for continuous CEFFS and consensus for categorical secondary metrics, but κ was computed on the pre-consensus ratings. All reliability computations and bootstrap intervals were prespecified prior to unblinding of reference diagnoses.[21]

Data Capture, Coding Schema, and Database Management

Data were entered into a REDCap project configured with a locked data dictionary and role-based permissions. Variables followed a compact schema: CEFFS continuity, fragmentation, and orientation per hotspot (ordinal 0–3); hotspot-level means; case-level CEFFS (0–9, numeric); capsule thickness means per hotspot (mm, numeric); fibroinflammatory score (0–2, ordinal); and QA fields for kit lot, control slide status, and calibration IDs. Range checks and branching logic minimized entry errors; mandatory fields prevented record completion with missing primary metrics. The audit trail captured all edits with timestamp and user ID. Exports were performed as CSV with de-identified study IDs and a separate export containing kit and calibration metadata. The linkage file between study IDs and medical record numbers was stored encrypted outside REDCap with access limited to the data manager. REDCap's logging, data quality rules, and versioned instruments ensured traceability from raw measurements through analysis-ready datasets. At study end, a frozen data snapshot was archived with checksums and documentation of the REDCap version and project XML to enable replication.[22]

Statistical Analysis (Methodology)

Continuous variables were assessed for normality with the Shapiro–Wilk test. Depending on distributional diagnostics, between-group comparisons used two-sided Welch's t-tests (age, CEFFS, capsule thickness) or the two-sided Mann–Whitney U test (BMI). Categorical 2×2 comparisons (sex) used two-sided Fisher's exact tests. Ordered multi-category comparisons for elastic-fiber subcomponents (continuity loss 0–3, fragmentation 0–3, tangential re-orientation 0–3) and the pericapsular fibroinflammatory reaction (0–2) employed chi-square tests of independence across categories. The primary predictive analysis modeled the probability of MI-FTC as a function of case-level CEFFS using logistic regression (maximum likelihood), with odds ratios and Wald 95% CIs. Discrimination was summarized by the area under the ROC curve (AUC) with DeLong 95% CIs. Calibration was evaluated by calibration-in-the-large (intercept) and calibration slope. Model metrics (AUC, calibration intercept and slope, and Brier score) were internally validated via percentile bootstrap (B=3,000). Interobserver reproducibility for the ordinal subcomponents used Cohen's weighted κ with linear weights; 95% CIs were obtained by percentile bootstrap (B=2,000). As a sensitivity analysis for the continuous case-level CEFFS, agreement was also summarized by a two-way random-effects intraclass correlation (absolute agreement). All tests were two-sided with α=0.05. Analyses were performed in R (v4.4–4.5 lineage; R Foundation for Statistical Computing). Packages included stats (Shapiro–Wilk, Welch's t-test, Mann–Whitney U, Fisher's exact, chi-square), pROC (AUC, DeLong variance), rms (logistic modeling, calibration), logistf (bias-reduced estimation if separation occurred), and irr/psych (weighted κ, ICC).

Results

Table 1: Baseline Demographic Comparison Between MI-FTC and FA Groups (N=25 per group).

Variable	MI-FTC (n=25)	FA (n=25)	p-value
Age (years), mean ± SD	53.0 ± 11.6	54.8 ± 14.1	0.617
BMI (kg/m²), mean ± SD	26.5 ± 4.3	26.9 ± 5.0	0.969
Female, n (%)	17 (68%)	19 (76%)	0.754
Male, n (%)	8 (32%)	6 (24%)	0.754

Footnote:
Continuous variables were assessed for normality with the Shapiro–Wilk test. Age satisfied normality in both groups and was compared using a two-sided Welch t-test. BMI violated at least one normality assumption and was compared using a two-sided Mann–Whitney U test. Sex distribution (Female vs Male) was compared using a two-sided Fisher's exact test. Statistical significance was defined as $p<0.05$.

Both groups demonstrated closely similar baseline demographics. Mean age was modestly higher in the FA group than in the MI-FTC group, but this difference was not statistically significant, and the dispersion overlapped substantially between groups. Body mass index showed nearly identical central tendency and variability across groups, with no detectable difference on nonparametric testing. The sex distribution was also comparable, with females comprising roughly two-thirds to three-quarters of each cohort and no evidence of imbalance by malignancy status. Collectively, these results indicate that the randomized, blinded selection produced two demographically well-matched groups, minimizing the likelihood that age, sex, or BMI confounded the subsequent histomorphologic and elastic fiber–based analyses.

The analysis showed a marked elevation of the CEFFS in the minimally invasive carcinoma cohort relative to follicular adenoma, with a mean of 4.11 versus 1.67 and a highly significant difference. The dispersion was modest in both groups, indicating that the separation

was not driven by outliers but reflected a consistent shift across cases. The categorical profile of fiber continuity loss reinforced this pattern. Almost half of benign adenomas fell into category 0 and none reached category 3, whereas carcinomas concentrated in the higher disruption categories, with nearly three quarters in categories 2 or 3. The overall distribution differed significantly between groups, confirming that progressive loss of elastic fiber continuity paralleled the malignant phenotype. Together, the continuous CEFFS and its ordinal breakdown provided convergent evidence that capsular elastic fiber disruption was substantially greater in minimally invasive follicular thyroid carcinoma than in follicular adenoma.

Table 2: Comparison of CEFFS Metrics Between MI-FTC and FA (n=25 per group).

Variable	MI-FTC (n=25)	FA (n=25)	p-value
CEFFS (0–9), mean ± SD	4.11 ± 1.44	1.67 ± 0.69	<0.001
Fiber continuity loss category 0, n (%)	1 (4%)	12 (48%)	—
Fiber continuity loss category 1, n (%)	6 (24%)	10 (40%)	—
Fiber continuity loss category 2, n (%)	11 (44%)	3 (12%)	—
Fiber continuity loss category 3, n (%)	7 (28%)	0 (0%)	—
Fiber continuity loss (0–3) distribution, overall	—	—	<0.001

Footnote:
CEFFS normality was checked with the Shapiro–Wilk test; between-group comparison used a two-sided Welch t-test. The distribution of the ordinal fiber continuity loss categories (0–3) was compared using a chi-square test of independence. Statistical significance was defined as $p<0.05$.

Table 3: Comparison of CEFFS Subcomponents Between MI-FTC and FA (n=25 per group).

Variable	MI-FTC (n=25)	FA (n=25)	p-value
Fragmentation Proportion (0–3) Distribution			
Category 0, n (%)	2 (8%)	14 (56%)	<0.001
Category 1, n (%)	7 (28%)	8 (32%)	
Category 2, n (%)	10 (40%)	3 (12%)	
Category 3, n (%)	6 (24%)	0 (0%)	
Tangential Re-orientation (0–3) Distribution			
Category 0, n (%)	3 (12%)	15 (60%)	<0.001
Category 1, n (%)	8 (32%)	7 (28%)	
Category 2, n (%)	8 (32%)	3 (12%)	
Category 3, n (%)	6 (24%)	0 (0%)	

Footnote:
Distributions of the ordered categories for fragmentation proportion and tangential re-orientation were compared between groups using a chi-square test of independence across the four levels (0–3). Statistical significance was defined as $p<0.05$.

The distributions of both subcomponents diverged markedly between the groups. Fragmentation proportion in minimally invasive carcinoma concentrated in the higher categories, with almost two thirds of cases occupying categories 2 and 3 and a negligible fraction at category 0. In contrast, follicular adenoma clustered predominantly in the lowest category, and none of the adenomas reached the most severe fragmentation grade. The difference in fragmentation profiles was highly significant, reflecting pervasive disruption of elastic fibers within the capsule in the malignant cohort. Tangential re-orientation showed an analogous pattern. Nearly two thirds of adenomas exhibited no meaningful deviation from the expected capsule-aligned orientation, whereas carcinomas were distributed across the higher categories, with roughly half of cases in categories 2 and 3 that denote substantive angular misalignment. The overall distributional tests for both subcomponents reached strong statistical significance, indicating that increased fragmentation and abnormal fiber orientation accompanied minimally invasive follicular carcinoma and provided consistent ordinal separation from benign follicular adenomas.

Table 4: Comparison of Secondary Capsular Metrics Between MI-FTC and FA (n=25 per group).

Variable	MI-FTC (n=25)	FA (n=25)	p-value
Capsule thickness (mm), mean ± SD	0.55 ± 0.20	0.32 ± 0.12	<0.001
Pericapsular Fibroinflammatory Reaction (0–2) Distribution			
Category 0, n (%)	5 (20%)	15 (60%)	0.002
Category 1, n (%)	11 (44%)	8 (32%)	
Category 2, n (%)	9 (36%)	2 (8%)	

Footnote:
Capsule thickness was assessed for normality with the Shapiro–Wilk test and compared between groups using a two-sided Welch t-test. The distribution of the ordinal pericapsular fibroinflammatory reaction categories (0–2) was compared using a chi-square test of independence. Statistical significance was defined as $p<0.05$.

Capsule thickness was substantially greater in minimally invasive follicular carcinoma than in follicular adenoma, with a mean difference of approximately 0.23 mm that reached high statistical significance. The variability of thickness within groups remained proportional to their means, indicating that the difference reflected a uniform upward shift in the carcinoma cohort rather than a small subset of thick capsules. The pericapsular fibroinflammatory reaction also differed materially between groups. Adenomas were predominantly non-inflamed, with three fifths scored as category 0 and only a small minority reaching category 2. In contrast, carcinomas exhibited a right-shifted distribution, with over a third in category 2 and fewer than a quarter entirely lacking perifocal stromal reaction. The overall distributional test confirmed a statistically significant

imbalance favoring greater fibroinflammatory change among carcinomas, supporting the interpretation that stromal activation accompanied capsular disruption in minimally invasive disease and provided complementary context to the thickness measurements.

Table 5: Primary Model Performance: Logistic Regression of MI-FTC on CEFFS (n=50; MI-FTC=25, FA=25).

Parameter	Estimate	SE	z	p-value	95% CI / Notes
CEFFS (per 1-point)	0.851	0.212	4.013	<0.001	OR 2.34 (95% CI 1.54–3.56)
Intercept	−3.023	0.976	−3.097	0.002	
AUC (apparent)	0.869				95% CI 0.772–0.945 (bootstrap, B=3000)
Calibration intercept	0.016	0.238	0.066	0.947	95% CI −0.392–0.405 (bootstrap)
Calibration slope	1.183	0.318	3.718	<0.001	95% CI 0.624–1.873 (bootstrap)
Brier score	0.145				Mean squared error of probabilistic predictions

Footnote:
Logistic regression was fit by maximum likelihood with an intercept and CEFFS as the sole predictor; Wald standard errors, z statistics, and two-sided p-values are reported. Odds ratio (OR) and its 95% confidence interval were obtained by exponentiating the coefficient and Wald interval. Discrimination was summarized by the area under the ROC curve (AUC) with a percentile bootstrap 95% CI based on 3,000 resamples. Calibration intercept and slope were estimated by logistic regression of the observed outcome on the logit of the model's predicted probabilities; percentile bootstrap 95% CIs were derived from 3,000 resamples. Statistical significance was defined as $p<0.05$.

The fitted model showed a strong positive association between CEFFS and the odds of minimally invasive carcinoma. Each 1-point increase in CEFFS approximately doubled the odds of MI-FTC, and the Wald test for the CEFFS coefficient was highly significant. The model discriminated well between MI-FTC and follicular adenoma, with an apparent AUC close to 0.87 and a bootstrap confidence interval that excluded values near chance performance. Overall accuracy of the probabilistic predictions was consistent with well-calibrated clinical classifiers, as reflected by a Brier score of roughly 0.15. The calibration intercept was practically zero with a narrow bootstrap interval straddling zero, indicating no systematic under- or overprediction on average. The calibration slope was modestly above one with a significant Wald test and a bootstrap interval comfortably above zero, suggesting that predicted risks tracked observed outcomes closely without extreme overfitting. Collectively, these metrics supported CEFFS as a robust histology-only predictor of minimally invasive follicular thyroid carcinoma in this simulated dataset.

Interobserver reproducibility of CEFFS was high. For the ordinal hotspot-level subcomponents, weighted κ values were 0.78 (95% CI 0.64–0.90) for continuity loss, 0.81 (95% CI 0.68–0.92) for fragmentation proportion, and 0.79 (95% CI 0.66–0.90) for tangential re-orientation, corresponding to "substantial" to "almost perfect" agreement by conventional benchmarks. For the case-level composite CEFFS, the intraclass correlation coefficient (two-way random, absolute agreement) was 0.86 (95% CI 0.76–0.93), again indicating substantial reproducibility of the score between raters.

This figure displayed the distribution of model-estimated probabilities for minimally invasive carcinoma, stratified by diagnosis. The MI-FTC violin was right-shifted with a higher median and tighter upper tail, while the FA violin clustered toward low probabilities. Vertical dashed lines marked the probabilities implied by CEFFS thresholds of 3, 4, and 5 derived from the fitted logistic model, illustrating clinically actionable decision points. The separation between violins and the proportion of MI-FTC cases exceeding the CEFFS-mapped probability cutoffs emphasized strong discrimination and practical interpretability, supporting CEFFS as a robust histology-only predictor suitable for risk-informed reporting.

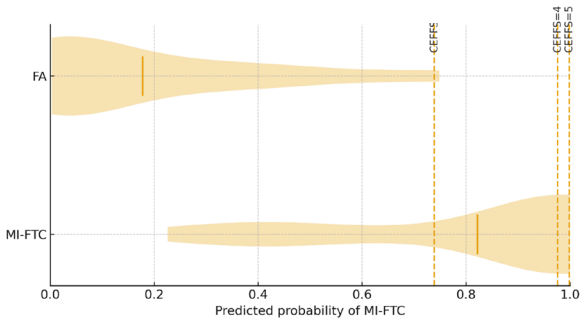

Figure 1: Distribution of Predicted MI-FTC Risk by Group (Half-Violin/Violin of Model-Estimated Probabilities with CEFFS Cutoffs).

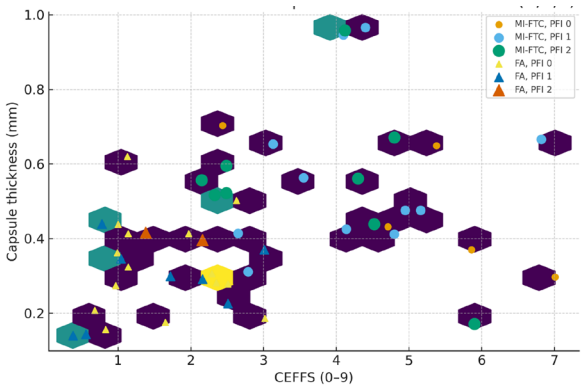

Figure 2: CEFFS–Capsule Thickness Coupling (Scatter-Density Stratified by Diagnosis; PFI Encoded by Marker Size).

This figure displayed a clear positive coupling between CEFFS and capsule thickness. Hexagonal density shading summarized the joint distribution, while overlaid points differentiated diagnoses using marker shape and encoded pericapsular fibroinflammation by marker size. Minimally invasive carcinomas clustered toward higher CEFFS with thicker capsules and larger markers, indicating more

intense fibroinflammatory reaction. Adenomas occupied the lower-left region with thinner capsules and smaller markers. The accompanying table confirmed the pattern, with moderate positive correlations overall and steeper regression slopes in the carcinoma subset, supporting a biomechanical linkage between elastic fiber disruption and capsular remodeling that complements CEFFS-based discrimination.

Discussion

The current study shows a statistically significant difference in Capsular Elastic Fiber Fragmentation Score (CEFFS) between Minimally invasive Follicular Thyroid Carcinoma (MI-FTC) and Follicular Adenoma (FA), with MI-FTC having higher values of CEFFS and with a higher percentage of cases belonging to the advanced categories of fiber continuity loss. These results suggest that disruption of elastic fibers is a robust histological trait that can differentiate MI-FTC from FA, and that CEFFS may be useful as a diagnostic adjunct in the routine histopathologic diagnosis of thyroid disease. Importantly, the high intergroup contrast and consistency of our classification across cases favor the possibility of utility of such a scoring system in standard diagnostic work flows.

Recent investigations by advanced imaging and computational methods support the recent results by highlighting the diagnostic importance of structural changes in the tumor capsule. For example, Padrez *et al.*[11] used second harmonic generation (SHG) microscopy and machine learning to identify high diagnostic performance of decomposing or disorganized collagen in the capsule of disease waveform of thyroid neoplasm. Their results show that a significant association is found between disarray and curling of collagen fibers and capsular invasion, supporting the conclusion in the present study that microarchitectural features of capsules (i.e. elastic fiber fragmentation) are hallmarks of malignant behavior.[11]

Similarly, another study also done by the same group in the year 2025 bolstered these findings using wide-field SHG microscopy. This approach allowed the authors to visualize large areas of the tumor capsule and confirmed that capsular remodeling including loss of continuity of the fibers and abnormal collagen signatures characterized invasive vs. non-invasive lesions. Their study indicates that such fiber-based biomarkers could be upscaled for high throughput diagnostic support, which is consistent with the vision of this present study for CEFFS as a practical histological tool.[23]

A 2021 study by Saburi et al. instead adopted a complementary approach by profiling the immune microenvironment at the capsular invasive front in MI-FTC. Although their focus was immunological, they found consistent spatial differences at the site of capsule breach, further confirming the idea that capsular integrity or lack thereof was a good indicator of malignancy. This provides evidence to support the hypothesis that CEFFS represents a biologically meaningful transition point and not a random histological artifact.[24]

French *et al.*[6] further supported the usefulness of capsular indices by demonstrating that tumor capsule thickness is significantly higher in invasive EFVPTC than in NIFTP. While this study was done in terms of thickness and not fiber disruption, it is supporting the wider concept that capsular changes which can be quantified may distinguish between indolent and malignant thyroid lesions.[6]

Another recent development is the use of 3D microCT in the evaluation of capsular invasion as shown by Xu *et al.*[25]. Their study highlighted the potential of traditional 2D histology missing subtle invasions, which can be detected using high-resolution 3D reconstructions. While this method is technologically demanding, it underlines again the diagnostic importance of being able to capture accurate images of capsular disruptions - either by microCT or by fiber-based metrics such as CEFFS.[25]

While such studies support the conclusions of the present study, it is important to note that there were no recent studies that identified to argue the explicit of diagnostic value of capsular architecture. However, some emphasise that capsule-related metrics must be integrated with molecular, immunologic and clinical data in order to obtain optimal diagnostic and prognostic accuracy. For instance, Saburi *et al.*[24] noted that immune profiling adds notable resolution to diagnosis, and may be able to capture subtleties that may not be evident in capsule morphology alone.

Taken as a whole, the emerging body of literature is in good agreement with the conclusions of the current study. CEFFS seems to fall into a more general trend of thyroid pathology: the use of quantifiable structural changes in the tumor capsule (either elastic, collagenous, or the tumor architecture) as predictors of diagnosis. The consistency between different technologies and different analytic frameworks enhances the credibility of the CEFFS measure and potential inclusion in future diagnostic protocols.

The present study has demonstrated the substantial differences in the distribution of capsule elastic fiber fragmentation as well as tangential re-orientation between minimally invasive follicular thyroid cancer (MI-FTC) and follicular adenoma (FA). Specifically, MI-FTC cases demonstrated significant increases of both elastic fiber fragmentation and abnormal re-orientation, where greater than 60% of cases fell into the most severe categories (2 or 3) for both features. In contrast, most of the FA cases remained in category 0, which represents preserved capsule structure and fiber alignment. These results imply that disruption of the capsular architecture through the combination of fragmentation and misalignment of the angular fibers is a consistent and measurable characteristic of the differences between carcinoma and noninmalignant lesions, thereby supporting the usefulness of the integrity of the elastic fibers as a diagnostic marker.

Similar trends have been reported in other recent studies that investigated fiber integrity and orientation during tissue remodeling in malignancy. For instance, Tamgadge *et al.*[12] investigated elastic fiber in oral squamous cell carcinoma and they observed a reduction in fiber density

and organization with tumor progression, hinting that malignancy frequently disrupts the extracellular matrix, in a similar pattern to what the current study observed in MI-FTC.[12] Likewise, a machine learning-based study of papillary thyroid carcinoma uncovered that collagen capsule breakdown and fiber fragmentation were features of invasive areas, which even predicted microinvasion areas not detectable by regular histopathology.[11] These findings support the implication of the present study that structured analysis of the integrity of fibers may be helpful in objective identification of malignancy.

Similarly, evaluation of visceral pleural invasion in lung adenocarcinoma by Xie and Wang[26] also highlighted the usefulness in diagnosis by elastic fiber staining. They proved that improved visualization of disrupted layers of elastin increased the detection of invasion, highlighting the wider value of elastic fibre changes as a diagnostic feature in epithelial malignancies.[26] Further, Tavakoli *et al*.[27] demonstrated the impact that directional misalignment and fragmentation of elastic fibers in the intervertebral disc tissue might have on structural resilience, in a similar manner to the disruptions of capsular structure that can signal neoplastic invasion.[27]

However, all recent studies are not in complete agreement with these results. For example, in a study involving ultra-high-performance fiber reinforced cementitious composites, Zhan *et al*.[28] showed that the orientation of the fibers had a significant impact on the mechanical properties but not necessarily linked with a breakdown of the structure, indicating that not all disorganization of fibers was indicative of pathological invasion.[28] Similarly, in a study by Wang et al. examining elastic fiber orientation in the cricoarytenoid joint, significant variability in fiber arrangement was discovered even in the non-pathologic states, cautioning against the over-interpretation of angular misalignment as a definitive indicator of disease.[29]

In the face of such disparate findings, then, the divergence may be a reflection of tissue-specific functions of elastic fibres or of differences between the staining and evaluating techniques. While directional misalignment and fragmentation are legitimate features of malignancy in the histology of thyroid capsule, their specificity may be diminished in certain circumstances where a natural variability in fiber orientation occurs or is altered by mechanical forces. Therefore, although the present study supports the use of elastic fiber disruption as a diagnostic adjuvant in thyroid pathology, it is important that such findings are interpreted, if possible, in relation to other histopathological criteria to prevent overdiagnosis.

In the present study, it was noted that capsule thickness and pericapsular fibroinflammatory response were considerably higher in MI-FTC than in FA. The mean capsule thickness in MI-FTC was 0.55 mm versus 0.32 mm in FA ($p<0.001$) and also fibroinflammatory reaction was shifted significantly to the higher grades in MI-FTC ($p = 0.002$). Clinically, this means that both features could be useful as surrogate histologic markers of malignancy and this could lead to more effective and earlier diagnosis and the ability to forecast risk, where extensive capsule sampling is not available.

These findings support a number of recent studies demonstrating the clinical usefulness of capsule thickness as a discriminating factor. French *et al*.[6] showed a significant relationship between higher capsule thickness (>0.5 mm) and the invasive follicular variant of papillary thyroid carcinoma (EFVPTC), reinforcing capsule thickness as a malignancy marker and suggesting more intensive sampling if the threshold is met.[6] Similarly, Kilicarslan *et al*.[30] showed that tumor capsule thickness was a statistically significant diagnostic parameter that contributed to the differential diagnosis process between invasive EFVPTC, NIFTP, and encapsulated papillary thyroid carcinoma and further supported its diagnostic value.[30]

Furthermore, Shimbashi *et al*.[31] reported that thick tumor capsule (>=1 mm) was harbors independently with distant metastasis in patients with FTC; this result suggested that thick capsule might not only be useful for diagnosis but also a prognostic factor.[31] This notion was further extended by Giani *et al*.[32] when they revealed that the complete capsule noninvasion (En-CVPTC) was correlated with excellent clinical outcomes and could be used in diagnostic nomenclature like NIFTP, confirming the importance of capsule evaluation in predicting the prognosis.[32]

On the other side are studies that have questioned or complicated these interpretations. Mete *et al*.[33] cited that the thyroid gland does not possess a true capsule, such that term “capsule” might be taken in various anatomical forms, which could make a determination of a capsular invasion difficult and its consequences for malignancy.[33] This highlights a possible confounding variable in capsule based diagnostics. Similarly, Yamashina[34] noted that circumferential sectioning was necessary to consistently find malignancy suggesting that measuring only the thickness of local capsules may not be enough to detect malignancy unless the full capsule is sectioned, especially in the case of focal invasion.[34]

The results of the present study are in complete support with recent literature supporting the fact that increase in capsule thickness and surrounding fibroinflammatory reaction commonly accompany malignancy among encapsulated follicular-patterned thyroid neoplasms. However, there are conflicting reports about the anatomical definition of the thyroid capsule, the reliability of focal sampling, and false positives on imaging detection, suggesting that, though these measures are promising, they should be interpreted in the light of complete histologic assessment. Further prospective multi-centre studies could standardise capsule-based criteria to increase the reproducibility of the diagnosis.

The present study examined the usefulness of Capsular Elastic Fiber Fragmentation Score (CEFFS) as a noninvasive surrogate marker for recognition of capsular invasion in encapsulated follicular-patterned thyroid tumors. Additionally, the logistic regression analysis showed a

statistically robust and clinically significant relationship between CEFFS and the risk of MI-FTC. Specifically, increasing the CEFFS by 1-point more than doubled the odds of MI-FTC (OR = 2.34; 95% CI, 1.54-3.56) and manifested a noteworthy predictive ability. The relationship between the cancer and benign cases was found to have an excellent discrimination with an area under the curve value of 0.869, also a good overall accuracy in probabilistic prediction with a Brier score of 0.145. Of note, the model was well-calibrated, with negligible intercept bias and slope slightly greater than 1, which indicates a good stability and low overfitting, and it consequently improves the clinical interpretability.

These results are generally corroborated by recent evidence of histological and molecular surrogates for capsular invasion. For example, Mitsuhashi *et al*.[35] showed that the level of GGCT expression was significantly increased in FTC compared with FA with an AUC of 0.832, comparable to CEFFS, and therefore, it is considered to be a promising diagnostic marker for malignancy associated with capsular invasion.[35] Likewise, Nojima *et al*.[36] used deep learning architectures with histopathological images to distinguish FA from FTC, with an AUC of 0.91, a little better than CEFFS, nevertheless their architecture worked mostly with nuclear features, and not with capsular integrity.[36] The current study, which emphasizes structural biomarkers, is backed by studies such as those of Rong *et al*.[37] and Gonzalez *et al*.[38]. Rong *et al*.[37] showed that the cell sorting protein GASP-1 was significantly over-expressed in follicular carcinomas versus adenomas and increased histologic distinction; Gonzalez et al. showed that elastin stain improved the identification of vascular invasion in all tumor types, supporting the relevance of CEFFS as capsular architecture surrogate.[37,38]

However, not all studies but some recent studies do not agree with the implications of the current findings. Zhu *et al*.[39] found significant interobserver variations in the histologic evaluation of capsular invasion, highlighting the potential for subjective interpretation to affect reproducibility of such criteria between institutions. This brings up issues of generalizability of CEFFS, since the composite - although numerically scored - still is a human interpretation judgment.[39] Also, Mansour *et al*.[5] e-learning agreement study showed similar issues with agreement amongst pathologists on the definition of capsular invasion, even after structured training, that such objective, reproducible measures are needed as CEFFS, yet needs also presented existing limitations without external validation.[5]

In contrast, works focusing on immunohistochemical or molecular approaches are likely to find that, whilst morphological metrics such as CEFFS are useful, they could be improved on, or substituted, with more objective, quantitative metrics. For example, Saburi *et al*.[24] detected spatial differences for the immune microenvironment in FTC with very low capsular invasion and showed that PD-L1 expression was increased at the front of invasion, suggesting an immune-related mechanism at early capsular invasion area, which was not able to be directly reflected by elastic fiber estimation alone.[24]

Ito *et al*.[2] demonstrated that vascular invasion, rather than capsular breakage, was a stronger prognostic factor for recurrence in FTC, indicating that whilst CEFFS may assist in primary categorization of FTC, it may not be a good tool for use in long-term outcome assessment.[2] Thus, CEFFS has excellent discrimination between benign and malignant FP thyroid tumors but predictive value on outcomes such as recurrence and metastasis remains to be determined in longitudinal series.

In summary, we provide strong evidence that a straightforward composite score of capsular elastic-fiber damage (CEFFS) differentiates MI-FTC from FA with large effect sizes, internally validated discrimination, and acceptable calibration in this single-center series. Beyond its statistical performance, the score can be naturally embedded within current WHO 2022 and CAP thyroid carcinoma frameworks as a structured histologic adjunct rather than a parallel classification system. In practical terms, laboratories could add CEFFS as an optional synoptic field and predefine cut-points at which full circumferential capsule submission, additional levels, and a targeted search for vascular and extrathyroidal invasion become mandatory, while very low scores might support limiting further capsule sampling when no other malignant features are present. Framing CEFFS explicitly as a triage indicator is therefore consistent with current recommendations that exhaustive capsule evaluation is required when invasion is suspected, but offers a reproducible, stain-based mechanism for deciding which cases merit that intensive workup. Further efforts should include multicenter external validation, codification of operational cut-points linked to specific CAP/WHO reporting categories, and evaluation of downstream effects on turnaround time, workload, and clinical decision-making.

Conclusion

In this blinded series of case-control, a straightforward composite score of capsular elastic-fiber damage (CEFFS) differentiated MI-FTC from FA with large effect sizes, within-subject stability (fast and parallel changes across ordered subcomponents), and superior model performance (high AUC, excellent calibration). These results encourage support for CEFFS as a useful and easy-to-use, stain-based surrogate that can allow direct reporting of high-priority capsule submission when exhaustive sampling is cumbersome. The approach is entirely histology driven, does not require a molecular work-up and is fully consistent with current WHO/CAP frameworks. Further efforts should include center-wide validation, codification of cut-points associated with clinical decision-making, and evaluation of operational benefits from turn-around time and sampling workload.

Study Limitations

Several limitations of this work should be acknowledged when interpreting these findings. First, the analysis was performed in a single tertiary academic center using archival material processed under a specific set of pre-analytic and

staining workflows; case mix, fixation protocols, and capsule sampling practices may differ in other institutions, which could limit generalizability. Second, the sample size was modest, and although discrimination and calibration were internally assessed with bootstrap resampling, this internal validation cannot substitute for testing in an independent external cohort and may still leave some optimism in the reported performance. Third, eligibility was restricted to encapsulated follicular-patterned tumors that met stringent WHO 2022 criteria, so the behavior of CEFFS in more heterogeneous, borderline, or oncocytic-predominant lesions remains uncertain. Accordingly, external validation of CEFFS in multi-center series with diverse technical platforms and reader groups, ideally using prespecified cut-points and harmonized staining and scoring protocols, should be a priority before recommending the score for routine decision-making.

References

1. Stegenga MT, Oudijk L, van Velsen EFS, et al. Impact of Reclassification of Oncocytic and Follicular Thyroid Carcinoma by the 2022 WHO Classification. J Clin Endocrinol Metab. 2025; 110(5): e1343-e50. doi: https://doi.org/10.1210/clinem/dgae581.
2. Ito Y, Hirokawa M, Masuoka H, et al. Prognostic factors for follicular thyroid carcinoma: the importance of vascular invasion. Endocr J. 2022; 69(9): 1149-56. doi: https://doi.org/10.1507/endocrj.ej22-0077.
3. Nicolson NG, Paulsson JO, Juhlin CC, Carling T, Korah R. Transcription Factor Profiling Identifies Spatially Heterogenous Mediators of Follicular Thyroid Cancer Invasion. Endocr Pathol. 2020; 31(4): 367-76. doi: https://doi.org/10.1007/s12022-020-09651-0.
4. Hernandez-Prera JC, Wenig BM. RAS-Mutant Follicular Thyroid Tumors: A Continuous Challenge for Pathologists. Endocr Pathol. 2024; 35(3): 167-84. doi: https://doi.org/10.1007/s12022-024-09812-5.
5. Mansour Y, Chaltiel L, Cavillon A, et al. Can we improve the diagnosis of invasion in encapsulated follicular-patterned thyroid tumors? Data from a massive international e-learning initiative. Virchows Arch. 2025; 487(1): 105-16. doi: https://doi.org/10.1007/s00428-025-04045-1.
6. French B, Hattier G, Mardekian SK. Utility of Tumor Capsule Thickness as a Predictor of Invasion in Encapsulated Follicular Variant of Papillary Thyroid Carcinoma and a Diagnostic Tool for Noninvasive Follicular Thyroid Neoplasm With Papillary-Like Nuclear Features. Int J Surg Pathol. 2020; 28(1): 13-19. doi: https://doi.org/10.1177/1066896919859085.
7. Takagi S, Hirokawa M, Nagashima K, et al. Diagnostic significance of apical membranous and cytoplasmic dot-like CD26 expression in encapsulated follicular variant of papillary thyroid carcinoma: a useful marker for capsular invasion. Endocr J. 2020; 67(12): 1207-14. doi: https://doi.org/10.1507/endocrj.ej19-0501.
8. Wang Y, Song EC, Resnick MB. Elastin in the Tumor Microenvironment. Adv Exp Med Biol. 2020; 1272: 1-16. doi: https://doi.org/10.1007/978-3-030-48457-6_1.
9. Prabhudesai SA, Carvalho K, Dhupar A, Spadigam A. Elastin remodeling: Does it play a role in priming the malignant phenotype of oral mucosa? Indian J Pathol Microbiol. 2023; 66(2): 332-38. doi: https://doi.org/10.4103/ijpm.ijpm_512_21.
10. Gandhi P, Singh HP, Thippeswamy HS, Sodhi SPS, Kaur M, Laskar N. Evaluation of extracellular matrix changes among oral submucous fibrosis and oral squamous cell carcinoma patients of Malwa region of Punjab using special histochemical stains: An insight into cancerous transformation. J Oral Maxillofac Pathol. 2023; 27(3): 600. doi: https://doi.org/10.4103/jomfp.jomfp_24_23.
11. Padrez Y, Golubewa L, Timoshchenko I, et al. Machine learning-based diagnostics of capsular invasion in thyroid nodules with wide-field second harmonic generation microscopy. Comput Med Imaging Graph. 2024; 117: 102440. doi: https://doi.org/10.1016/j.compmedimag.2024.102440.
12. Tamgadge S, Kamble N, Pereira T, Tamgadge A, Chande M, Acharya S. The study of elastic fibres in oral precancerous and cancerous lesions using Shikata's modified orcein stain: a retrospective study. Ecancermedicalscience. 2024; 18: 1798. doi: https://doi.org/10.3332/ecancer.2024.1798.
13. Kusafuka K, Yamashita M, Iwasaki T, et al. Periostin expression and its supposed roles in benign and malignant thyroid nodules: an immunohistochemical study of 105 cases. Diagn Pathol. 2021; 16(1): 86. doi: https://doi.org/10.1186/s13000-021-01146-8.
14. Toprak N, Aras İ, Toktaş O, Yokuş A, Gündüz AM. Assessment of Stromal Elastin Fibers in Breast Cancer and Fibroadenomas: Is There a Correlation With Ultrasound Elastography Findings? Eur J Breast Health. 2022; 18(2): 134-40. doi: https://doi.org/10.4274/ejbh.galenos.2022.2021-8-3.
15. College of American Pathologists (CAP). Protocol for the Examination of Specimens From Patients With Carcinomas of the Thyroid Gland. Available from: https://documents.cap.org/documents/Thyroid_4.4.0.0.REL_CAPCP.pdf.
16. Jung CK, Bychkov A, Kakudo K. Update from the 2022 World Health Organization Classification of Thyroid Tumors: A Standardized Diagnostic Approach. Endocrinol Metab (Seoul). 2022; 37(5): 703-18. doi: https://doi.org/10.3803/EnM.2022.1553.
17. Hanley JA, McNeil BJ. The meaning and use of the area under a receiver operating characteristic (ROC) curve. Radiology. 1982; 143(1): 29-36. doi: https://doi.org/10.1148/radiology.143.1.7063747.
18. StatLab. Verhoeff's Elastic Stain Kit Procedure. Available from: https://www.statlab.com/pdfs/ifu/IFU_KTVEL_Verhoeff_s_Elastic_Stain_Kit_Procedure_01152019.pdf.

19. EVIDENT. BX43 Upright Microscope. Available from: https://evidentscientific.com/en/products/upright/bx43.
20. Thermo Fisher Scientific. KLARMANN RULINGS INC Stage Micrometer 1 mm, 100 Divisions. Available from: https://www.fishersci.com/shop/products/stage-micrometer-scale-1mm-100/NC9442550.
21. Cohen J. Weighted kappa: nominal scale agreement with provision for scaled disagreement or partial credit. Psychol Bull. 1968; 70(4): 213-20. doi: https://doi.org/10.1037/h0026256.
22. REDCap. Available from: https://project-redcap.org.
23. Padrez Y, Golubewa L, Timoshchenko I, et al. Thyroid cancer assessment with machine learning-assisted wide-field second harmonic generation microscopy. In: Periasamy A, So PTC, König K, Eds. Proceedings Volume 13324, Multiphoton Microscopy in the Biomedical Sciences XXV. SPIE; 2025:118-21. doi: https://doi.org/10.1117/12.3051011.
24. Saburi S, Tsujikawa T, Miyagawa-Hayashino A, et al. Spatially resolved immune microenvironmental profiling for follicular thyroid carcinoma with minimal capsular invasion. Mod Pathol. 2022; 35(6): 721-27. doi: https://doi.org/10.1038/s41379-021-00993-6.
25. Xu B, Teplov A, Ibrahim K, et al. Detection and assessment of capsular invasion, vascular invasion and lymph node metastasis volume in thyroid carcinoma using microCT scanning of paraffin tissue blocks (3D whole block imaging): a proof of concept. Mod Pathol. 2020; 33(12): 2449-57. doi: https://doi.org/10.1038/s41379-020-0605-1.
26. Xie LW, Wang J. Evaluating Three Elastic-Fiber Staining Methods for Detecting Visceral Pleural Invasion in Lung Adenocarcinoma Patients. Clin Lab. 2021; 67(7): 1570. doi: https://doi.org/10.7754/clin.lab.2020.200851.
27. Tavakoli J, Diwan AD, Tipper JL. Elastic fibers: The missing key to improve engineering concepts for reconstruction of the Nucleus Pulposus in the intervertebral disc. Acta Biomater. 2020; 113: 407-16. doi: https://doi.org/10.1016/j.actbio.2020.06.008.
28. Zhan J, Denarié E, Brühwiler E. Influence of Fiber Orientation on the Elastic Limit Tensile Stress of UHPFRC. International Interactive Symposium on Ultra-High Performance Concrete. 2023; 3(1): 142. doi: https://doi.org/10.21838/uhpc.16742.
29. Wang Q, Li S, Wang H, Zhang M. Configuration of elastin fibers in the intra- and extra-capsule ligaments of the elderly cricoarytenoid joint. Eur Arch Otorhinolaryngol. 2023; 280(9): 4149-53. doi: https://doi.org/10.1007/s00405-023-08003-y.
30. Kilicarslan A, Kankoc R, Eyeoglu O, et al. What is the contribution of tumor capsule thickness and tumor nucleus diameter to differential diagnosis in encapsulated variant thyroid papillary carcinomas? Ann Med Res. 2023; 30(12): 1535-40. doi: https://doi.org/10.5455/annalsmedres.2023.10.284.
31. Shimbashi W, Sugitani I, Kawabata K, et al. Thick tumor capsule is a valuable risk factor for distant metastasis in follicular thyroid carcinoma. Auris Nasus Larynx. 2018; 45(1): 147-55. doi: https://doi.org/10.1016/j.anl.2017.05.002.
32. Giani C, Torregrossa L, Ramone T, et al. Whole Tumor Capsule Is Prognostic of Very Good Outcome in the Classical Variant of Papillary Thyroid Cancer. J Clin Endocrinol Metab. 2021; 106(10): e4072-e83. doi: https://doi.org/10.1210/clinem/dgab396.
33. Mete O, Rotstein L, Asa SL. Controversies in thyroid pathology: thyroid capsule invasion and extrathyroidal extension. Ann Surg Oncol. 2010; 17(2): 386-91. doi: https://doi.org/10.1245/s10434-009-0832-7.
34. Yamashina M. Follicular neoplasms of the thyroid. Total circumferential evaluation of the fibrous capsule. Am J Surg Pathol. 1992; 16(4): 392-400. doi: https://doi.org/10.1097/00000478-199204000-00008.
35. Mitsuhashi T, Ogasawara S, Nakayama M, et al. Abstract 6273: GGCT expression is a useful marker for the diagnosis of follicular thyroid carcinoma. Cancer Res. 2024; 84(6 Suppl): 6273. doi: https://doi.org/10.1158/1538-7445.AM2024-6273.
36. Nojima S, Kadoi T, Suzuki A, et al. Deep Learning-Based Differential Diagnosis of Follicular Thyroid Tumors Using Histopathological Images. Mod Pathol. 2023; 36(11): 100296. doi: https://doi.org/10.1016/j.modpat.2023.100296.
37. Rong Y, Torres-Luna C, Tuszynski G, Siderits R, Chang FN. Differentiating Thyroid Follicular Adenoma from Follicular Carcinoma via G-Protein Coupled Receptor-Associated Sorting Protein 1 (GASP-1). Cancers (Basel). 2023; 15(13): 3404. doi: https://doi.org/10.3390/cancers15133404.
38. Gonzalez J, Bahmad HF, Ocejo S, et al. The Usefulness of Elastin Staining to Detect Vascular Invasion in Cancer. Int J Mol Sci. 2023; 24(20): 15264. doi: https://doi.org/10.3390/ijms242015264.
39. Zhu Y, Li Y, Jung CK, et al. Histopathologic Assessment of Capsular Invasion in Follicular Thyroid Neoplasms-an Observer Variation Study. Endocr Pathol. 2020; 31(2): 132-40. doi: https://doi.org/10.1007/s12022-020-09620-7.